ARL-AERO-REPORT-150

AR-001-335

DEPARTMENT OF DEFENCE

DEFENCE SCIENCE AND TECHNOLOGY ORGANISATION

AERONAUTICAL RESEARCH LABORATORIES

MELBOURNE, VICTORIA

AERODYNAMICS REPORT 150

PREDICTION OF HELICOPTER ROTOR DOWNWASH IN HOVER AND VERTICAL FLIGHT

by

K. R. REDDY

Approved for Public Release.

COPY No 10

JANUARY 1979

AR-001-335

DEPARTMENT OF DEFENCE
DEFENCE SCIENCE AND TECHNOLOGY ORGANISATION
AERONAUTICAL RESEARCH LABORATORIES

AERODYNAMICS REPORT 150

PREDICTION OF HELICOPTER ROTOR DOWNWASH IN HOVER AND VERTICAL FLIGHT

by

K. R. REDDY

SUMMARY

A method is presented for the calculation of rotor downwash in hovering and vertical flight. The blade is represented by a lifting line. The rotor wake is simulated by a vortex sheet and a series of rolled-up root and tip vortices, similar in form to that of a classical fixed-wing. The concept of rectangularization of the rotor wake is used in obtaining a formula for the normal component of induced velocity. Wake contraction based on experimental data is introduced into the calculations. Numerical calculations have been performed for two rotor configurations, viz. S-58 and a model rotor. Computed induced velocities and blade loadings are compared with the available flight data. The comparison shows the present simple method yields satisfactory results.

POSTAL ADDRESS: Chief Superintendent, Aeronautical Research Laboratories,
Box 4331, P.O., Melbourne, Victoria, 3001, Australia.

CONTENTS

NOTATION

a	lift-curve slope
A	wake contraction constant
b	number of blades
c	chord of the blade at station r
$\bar{c}$	ratio $0{\cdot}5\ ac/(R_2 - R_1)$
C_L	section lift coefficient
C_T	rotor thrust coefficient
h	distance between successive vortices
h_s	ratio $2sh/(R_2 - R_1)$
dl	lift on an element of the blade dr
m	radial station along the blade
M	total number of radial stations along the blade
N	number of rolled-up vortices
r	radial coordinate along the blade
R_r	position of root vortex
R_t	positions of tip vortex
R_1	inner radius of the blade
R_2	outer radius of the blade
s	number identifying the particular vortex under consideration
dT	thrust on an element of the blade dr
U_c	vertical velocity (+ ve up)
v_i	induced velocity (+ ve down)
v_o	mean induced velocity
v	induced velocity at P due to vortex sheet
v_s	induced velocity at P due to sth rolled-up vortex
W	incident velocity (see eqn. 5)
W_c	weight of the aircraft
α	incidence angle
Γ	circulation of station r
Γ_o	circulation round the centre of the aerofoil
η	integration variable (see eqn. 18)
θ	spanwise coordinate (see eqn. 16)
Θ	pitch of the blade at station r

k	wake contraction parameter
λ	velocity ratio (see eqn. 28)
ξ	offset ratio of lifting part of the blade (R_1/R_2)
ξ_r	ratio R_r/R_2
ξ_t	ratio R_t/R_2
ρ	air density
ϕ	integration variable (see eqn. 18)
Φ	inflow angle
Ψ	azimuth angle
Ω	angular velocity of rotor

1. INTRODUCTION

Rotor performance, blade motion stability, blade stresses, vibratory hub forces, aircraft stability and control, and aircraft flight simulation are some of the areas which require a knowledge of the non-uniform downwash at the rotor. In the flight simulation studies which are our main concern the rotor downwash is required in the calculation of rotor thrust and other rotor forces and moments. It is also needed in the calculation of aerodynamic forces on the helicopter fuselage, attached weapons and any other externally slung bodies. Probably one of the most difficult problems facing the rotary wing aerodynamicist at the present time is the determination of this induced velocity or rotor downwash. As each new generation of helicopters becomes more sophisticated, increased emphasis is put on improving the rotor induced velocity calculations.

The assumption that the distribution of induced velocity over the disc is uniform is thought to be satisfactory in forward flight when the flow through the rotor is large. In forward flight, with forward tilt of the rotor disc, the blades are moving away from the wake, therefore feeling less of its influence[1]. In the hovering case, however, the wake beneath the rotor may be expected to play a prominent part in determining the induced velocity. In this report, this important flight condition is the one analysed. A simple but rigorous analytical technique which will aid in understanding and interpreting the complex relationships between rotor circulation, downwash and blade motion will be of great value in helicopter flight simulation studies. This problem has been the subject of considerable work over many years. The calculation techniques have evolved from simple momentum theory based on actuator disc theory, through the classical blade element momentum method,[2] to wake modelling procedures. The advent of the high speed electronic digital computer has made possible the straightforward approach of tracing the vortex filaments trailed by each blade, and integrating the Biot-Savart relation to obtain induced velocities. The wake modelling methods progressed to the sophisticated and computationally demanding free wake analysis,[3-7] then retreated to the simpler prescribed wake[8-13] methods. In the prescribed wake method, the wake geometry is specified, on the basis of experimental data, as a function of rotor configuration and thrust level, through simple analytical expressions. In the free wake analysis the mutual interaction of the circulation distribution, downwash and blade motion is included. Many theoretical models based on the above free wake concept have been developed in Europe, United States of America and United Kingdom. The majority of these models rely exclusively on discrete vortex filament methods which are based on extensive digital computation. These techniques are necessary when detailed rotor blade airloads, vibration analysis, and acoustic properties[14] are required. However, because of the extensive numerical computations involved, they offer only limited physical insight, and lack the versatility of simpler methods. Even when using the most sophisticated models, convergence in the hovering range is very doubtful[3].

The aim of the following analysis is to develop a vortex-wake method for determining the induced velocity of a hovering helicopter. The method uses a simple, realistic wake model based on experimental data and Willmer's[15,16] mathematical simplification to avoid lengthy, complex computations. The basic geometry of the vortex-wake model is shown in Figure 1. In this model each blade is represented by a lifting line. The vorticity trailed by a rotor blade leaves the trailing edge in a sheet, which rolls up as a pair of concentrated tip and root vortices. In order to reduce the computational time, Willmer's principle of rectangularization is applied to the above wake model. Using this vortex-wake model, the calculated downwash distribution is compared with available theoretical and experimental results.

In developing the theory, consideration has been limited to aircraft having a single rotor. No restriction has been placed on the number of blades which the rotor may have, however. The aircraft has been assumed to be in steady vertical flight or hover. The fuselage interference on the rotor wake is not incorporated. It is also assumed that the fluid is inviscid and incompressible. The simplications employed in formulating the mathematical model restrict its

application to points in the rotor plane, but the model could be extended to include points in other regions of interest. The calculated rotor downwash may be used as a first approximation in the estimation of aerodynamic forces on the helicopter fuselage as well as any weapons attached to it.

2. ROTOR WAKE VORTICITY DISTRIBUTION

The underlying aerodynamic theory required will be better understood if the equivalent fixed wing problem shown in Figure 2 is first examined. Consider a wing advancing at constant angle of attack in a uniform airstream. By virtue of its geometrical angle of attack, the aerofoil will generate circulation and consequently lift. Assuming for simplicity that this circulation is constant along the span, it must leave the wing at the tips and trail downstream since, by one of the fundamental laws of hydrodynamics, circulation cannot end abruptly, but must continue back in a closed circuit to the starting vortex generated at the beginning of the motion. After the motion has continued for a sufficient length of time, this starting vortex may be assumed to be at an infinite distance from the aerofoil and its effects may be neglected. In practice of course the circulation is not constant along the span and therefore the trailing vortices are distributed in a sheet all along the span. Consider the case where the geometrical angle of attack changes as the wing advances. It is evident that the circulation will change but, since the total circulation must remain constant in the case of the ideal fluid, there must be a counter vortex in the wake corresponding to the change in circulation of the aerofoil. This wake vorticity is generally referred to as the shed vorticity to differentiate it from the trailing vorticity which occurs both in the steady state condition and when the angle of attack of blade is changing. In steady level flight, the variations in the angle of attack are small so that the magnitude of the resulting shed vorticity will also be small. Its contribution to the induced velocity is neglected. It is also well established that the vortex sheet behind an aerofoil is unstable and cannot persist.[17] The sheet tends to roll up somewhat like a sheet of paper as shown in Figure 2. Thus, at a sufficient distance behind the aerofoil, a section of the wake in a plane perpendicular to the direction of motion would show two cylindrical vortices whose distance apart is less than the span (refer to Fig. 9).

In Figure 1 the corresponding problem for the rotor is presented. Obviously the trailing wake does not disappear to infinity but returns underneath the rotor in a spiral form[18] and the very nature of this spiral prevents the development of simple solutions for the downwash which it induces at the blade. Because of this complexity, generalized solutions will probably never be possible for the problem. However, numerical solutions for specific cases are possible utilizing high speed digital computers. These solutions are frequently sufficient for engineering applications.

Figure 1 indicates pictorially the complexities of attempting to obtain a complete representation of the rotor wake. To solve this difficult problem numerically, Willmer made two simplifying assumptions. The first is that conditions change sufficiently slowly to allow a quasi-static approach. The second is that the spiral wake is amenable to rectangularization. Consider the trailing wake from a blade (Fig. 3). Willmer argued that the radius of curvature of the vortex sheet and rolled up vortices is large enough (especially for the important outer parts of the wake) for the wake elements (vortex sheet and rolled up vortices) to be regarded as straight. He also assumed that only those parts of the wake which are near to the reference blade are important. Consistent with this idea one may allow the rows of vorticity to extend to infinity in order to achieve mathematical simplification. Thus the wake attached to the reference blade is assumed to be a straight sheet extending back to infinity, while those of other blades are assumed to be doubly infinite rolled-up vortices as shown in Figure 4. The positions of these vortices depend on the mean flow velocity through the rotor disc, and the number and relative positions of the blades that shed them. Once the numbers and positions of the wake elements had been chosen, the induced velocity at the reference point could be calculated by an extension of Glauert's wing theory. Positioning of these vortices forms one of the important aspects in the calculations of induced velocity. The axial distance h between the vortices is calculated using the average induced velocity through the rotor. A method based on the experimental data is used to determine the radial locations. This is discussed in the following section.

3. WAKE GEOMETRY

The most important factor in the accurate calculation of rotor downwash today is the use of realistic wake geometry. Failure of most of the earlier classical performance prediction methods was attributed to the use of an uncontracted wake. In the following pages we briefly describe the wake geometry used in the present analysis.

Concurrently with the rotor inflow methods based on a theoretical wake geometry, other methods have been developed based on empirical wake models. Most of these methods are directed toward the rotor hover condition in that this condition is the one most influenced by wake distortion effects. The requirement for a method employing an accurate prescribed wake model derived from experimental wake data was concluded by Jenney, *et al*[11] who found that the rapid contraction of the slipstream under a hovering rotor places the vortex system sufficiently close to the rotor blades that it causes significant changes in the distribution of induced velocity. In the mid 1950's, Gray[8] developed a semi-empirical method for the wake of a single bladed rotor based on experimental wake geometry data obtained from smoke visualization tests. More recently, Landgrebe,[9] and Kocurek and Tangler[10] have conducted a series of smoke tests which confirm Gray's results and give more details of the wake geometry. Kocurek and Tangler measured wake shapes for 26 model rotor configurations described in Table 1.

TABLE 1
Model Rotor Configurations[10]

Blade linear twist (deg)	Aspect ratio	No. of Blades	Radius R_2 (m)	Chord c (mm)	ΩR_2 (m/s)
Untwisted Rotors					
0	7·1	1, 2, 3, 4	0·407	57·2	152·5
0	13·5	1, 2, 3	0·559	41·4	152·5
0	18·2	1, 2, 3, 4	0·680	37·3	152·5
Twisted Rotors					
11·0	13·5	1, 2, 4	0·559	41·4	152·5
11·3	8·0	1, 2, 4	0·458	57·2	152·5
16·0	7·1	1, 2, 4	0·407	57·2	152·5
18·0	8·0	1, 2, 4	0·458	57·2	152·5
24·0	7·1	1, 2, 4	0·407	57·2	152·5

All the blades had a rectangular plan form and a NACA 0012 airfoil section. Landgrebe obtained the wake geometry characteristics for all combinations of the rotor parameters given in Table 2.

TABLE 2
Values of Primary Test Parameters[9]

Number of blades	2, 4, 6, 8
Blade linear twist (deg)	0, 8, 16
Blade aspect ratio	13·6, 18·2
Rotor tip speed (m s)	160, 183, 214
Collective pitch*	0 to max†

* Value at r equal to 0·75 R_2

† Determined by operating stall limits.

The above two flow visualization studies revealed that the wake radial contraction occurs in an exponential manner with increasing wake azimuth, ψ. It is characterized by a rate parameter, k, and an effective minimum nondimensional radius, A. The generalized wake radial coordinate is given by

$$\frac{r}{R_2} \quad A \cdot (1 \quad A)\, e^{-k\psi} \tag{i}$$

For the stable near-wake region, the radial coordinates may be determined by substitution of the following combination of A and k in the above equation (i).

$$A \quad 0{\cdot}78$$

$$k \quad \begin{cases} 0{\cdot}145 \cdot 27{\cdot}0\, C_T & \text{Landgrebe} \\ 4{\cdot}0\,(C_T)^2 & \text{Kocurek and Tangler} \end{cases} \tag{ii}$$

Landgrebe's linear variation of k agrees with the non-linear representation of Kocurek and Tangler in the medium C_T range. However, in the case of the latter authors the contraction rate tends towards zero as the blade is unloaded. From the above equation (ii) it is concluded that for a given azimuth, the radial coordinate of the wake is a function of disc loading (or C_T) and decreases with increasing loading. For a fixed disc loading the radial coordinates are independent of tip speed, number of blades, blade twist, and aspect ratio. Taking a mean C_T value of 0·005 and h/R_2 equal to 0·058, the wake geometry is plotted in Figure 5. The Figure shows how rapidly the wake contracts under the rotor: the contraction is practically complete within a distance of 20 to 30 percent of the rotor radius.

Using the above described wake flow model and the wake contraction rate given by Kocurek and Tangler, a mathematical analysis is developed in the following section. The variation of the circulation with radius and the resulting downwash distribution is represented by a Fourier series. Unfortunately, since the loading of a rotor blade is very different from the elliptic loading of a conventional fixed wing, a large number of spanwise points are needed for acceptable accuracy. This means a large number of terms in the Fourier series, and this makes for lengthy computing times.

4. MATHEMATICAL FORMULATION

When a wing experiences lift, the pressure on its upper surface must be less than on its lower surface. It follows from Bernoulli's theorem that the velocity is higher over the upper surface than over the lower surface, and we should therefore expect that the circulation round a circuit surrounding the aerofoil would be non-zero. Following the lifting-line practice, the lift of an element of the blade dr and at a distance r from the origin is[17]

$$dL \quad \Gamma \rho W\, dr \tag{1}$$

When the inflow angle (the direction of flow relative to the blade) as shown in Figure 6 is small we can write

$$dT \quad \Gamma \rho W\, dr \tag{2}$$

In the above relationship neither thrust nor induced velocity are known. To obtain a further relationship, we now consider the lift characteristics of the blade where the blade is regarded as an aerofoil. The calculations follow closely the standard methods of aerofoil theory but the rotor analysis is simplified considerably because the blade incidence and inflow angles are usually sufficiently small that the familiar small angle approximations may be made.

Consider an element of blade of chord c with width dr at a radius r from the axis of rotation. The geometric pitch angle of the blade element relative to the plane of rotation is Θ, the climbing speed is U_c and the local induced velocity is v_i. The direction of the flow relative to the blade makes an angle Φ (usually called inflow angle) with the plane of rotation, and is given by (refer to Fig. 6)

$$\tan \Phi = (U_c + v_i)/\Omega r \tag{3a}$$

$$\text{or } \Phi \approx (U_c + v_i)/\Omega r \text{ for small } \Phi \tag{3b}$$

The lift on the blade element is

$$dL = \tfrac{1}{2} \rho W^2 c C_L \, dr \tag{4}$$

where

$$W = [(U_c + v_i)^2 + \Omega^2 r^2]^{\frac{1}{2}} \tag{5a}$$

and

$$W \approx \Omega r \tag{5b}$$

for small Φ

Let us suppose that the lift slope, a, of the section is constant so that, if the section incidence α is measured from the no-lift line, we can write

$$C_L = a\alpha = a(\Theta - \Phi) \tag{6}$$

The elementary lift is now

$$dL = \tfrac{1}{2}\rho \Omega^2 r^2 a(\Theta - \Phi) c \, dr \tag{7}$$

Using eqn. (3b) and assuming $dL \approx dT$

$$dT = \tfrac{1}{2} \rho a c \Omega^2 r^2 [\Theta - (U_c + v_i)/\Omega r] \, dr \tag{8}$$

Thus from eqns. (2) and (8) the relation between the circulation and the induced velocity becomes

$$\Gamma = \tfrac{1}{2} a c (\Theta \Omega r - U_c - v_i) \tag{9}$$

As in the fixed-wing case, the circulation round the rotor blade will vary across the span. Between the points η and $(\eta + d\eta)$ of the span of the blade, the circulation changes by the amount $-d\Gamma/d\eta \, d\eta$ and hence a trailing vortex of this strength springs from the element $d\eta$ of the span as shown in Figure 7.

The normal induced velocity at any point P along the span must be obtained as the sum of the effects of all the trailing vortices immediately behind the blade. The induced velocity due to the trailing vortex sheet is[19]

$$v_{sheet} = \frac{1}{4\pi} \int_{R_1}^{R_2} \frac{d\Gamma}{d\eta} \frac{d\eta}{r - \eta} \tag{10}$$

The next contribution comes from the rolled-up vortices stacked below the rotor blade near the root and tip as shown in Figure 8. The induced velocity perpendicular to the blade at P due to an element of rolled-up vorticity in the s'th wake at Q and Q' is[19]

$$v_s = \frac{1}{2\pi} \frac{(r - R_t)\Gamma_0}{(r - R_t)^2 + s^2 h^2} + \frac{1}{2\pi} \frac{(r - R_r)\Gamma_0}{(r - R_r)^2 + s^2 h^2} \tag{11}$$

so that the total for the whole wake is

$$\Sigma v_s \quad \frac{1}{2\pi}\sum_{s=1}^{s}\left[\frac{(r \quad R_t)\,\Gamma_0}{(r \quad R_t)^2 + s^2h^2} \quad \frac{(r \quad R_r)\,\Gamma_0}{(r \quad R_r)^2 + s^2h^2}\right] \tag{12}$$

Thus the total induced velocity at P perpendicular to the tip-path plane, which is given by that due to the immediate wake plus the sum of the contributions of the rolled-up vortices beneath the rotor, is

$$v_i \quad v_{sheet} + \Sigma v_s \tag{13}$$

From eqns. (9), (10), (12) and (13) the relation for the circulation Γ becomes

$$\Gamma \quad \tfrac{1}{2}ac\left\{\Theta\,\Omega r \quad U_c \quad \frac{1}{4\pi}\int_{R_1}^{R_2}\frac{dr}{d\eta}\,d\eta \quad \frac{1}{2\pi}\sum_{s=1}^{s}\left[\frac{(r \quad R_r)\,\Gamma_0}{(r \quad R_r)^2 + s^2h^2} \quad \frac{(r \quad R_t)\,\Gamma_0}{(r \quad R_t)^2 + s^2h^2}\right]\right\} \tag{14}$$

We now express the circulation in Fourier series form:

$$\Gamma \quad \Omega R_2(R_2 \quad R_1)\sum_{m=1}^{s} A_m \sin m\theta \tag{15}$$

where θ is defined by the relation

$$r \quad \left(\frac{R_2 + R_1}{2}\right) \quad \left(\frac{R_2 \quad R_1}{2}\right)\cos\theta \tag{16}$$

The integral in eqn. (14) is singular in nature. To evaluate it we use the well known result[17]

$$\int_0^{\pi}\frac{\cos m\phi\,d\phi}{\cos\phi \quad \cos\theta} \quad \frac{\pi\sin m\theta}{\sin\theta} \tag{17}$$

The relation between the variable η in eqn. (14) and ϕ in eqn. (17) is

$$\eta \quad \left(\frac{R_2 + R_1}{2}\right) \quad \left(\frac{R_2 \quad R_1}{2}\right)\cos\phi \tag{18}$$

Using eqns. (15) to (18), eqn. (14) reduces to

$$\sum_{m=1}^{\infty} A_m \sin m\theta \quad \frac{ac}{2(R_2 + R_1)}\left[\Theta\frac{r}{R_2} \quad \frac{U_c}{\Omega R_2} \quad \frac{1}{2}\sum_{m=1}^{s} m A_m \frac{\sin m\theta}{\sin\theta}\right.$$
$$\left. \frac{1}{\Omega R_2}\frac{1}{2\pi}\sum_{s=1}^{s}\left\{\frac{(r \quad R_r)\,\Gamma_0}{(r \quad R_r)^2 + s^2h^2} \quad \frac{(r \quad R_t)\,\Gamma_0}{(r \quad R_t)^2 + s^2h^2}\right\}\right] \tag{19}$$

The next step is to determine Γ_0, R_t and R_r. We use the theory developed by Glauert for a fixed wing aerofoil shown in Figure 9. The trailing vortex sheet behind an aerofoil is unstable and rolls up into a pair of vortices whose distance apart l' is rather less than the span l of the aerofoil. There is no established method the calculate to strength of the trailing vortices springing from an unsymmetrically loaded blade. Here we assume that the strength of these trailing vortices will be equal to the magnitude of the circulation Γ_0 round the centre of the aerofoil. If the form of load distribution across the span is represented as in equation (15) by the Fourier Sine series, then

$$\Gamma_0 \quad \Omega R_2(R_2 \quad R_1)\sum_{n=0}^{\infty} A_{2n+1}(-1)^n \tag{20}$$

and[19]

$$\frac{l'}{l} = \frac{\pi}{4} A_1 \sum_{n=0}^{\infty} A_{2n+1}(-1)^n = \frac{R_t - R_r}{R_2 - R_1} \tag{21}$$

From the wake geometry we also know the value R_t. Using the relation (21) we could calculate R_r the position of the rolled-up root vortex. Substituting eqn. (20), eqn. (19) reduces to

$$\sum_{m=1}^{\infty} \left(\sin m\theta + \frac{m\bar{c} \sin m\theta}{2 \sin \theta} \right) A_m - \frac{\bar{c}}{\pi} \sum_{s=1}^{\infty} \left[\begin{pmatrix} \frac{1+\xi}{1-\xi} - \cos\theta - \frac{2\xi_t}{1-\xi} \end{pmatrix} \quad \begin{pmatrix} \frac{1+\xi}{1-\xi} \quad \cos\theta - \frac{2\xi_r}{1-\xi} \end{pmatrix} \right] \sum_{n=0}^{\infty} A_{2n+1}(-1)^n$$

$$\begin{pmatrix} \frac{1+\xi}{1-\xi} - \cos\theta - \frac{2\xi_t}{1-\xi} \end{pmatrix}^2 + h_s^2 \quad \begin{pmatrix} \frac{1+\xi}{1-\xi} \quad \cos\theta - \frac{2\xi_r}{1-\xi} \end{pmatrix}^2 + h_s^2$$

$$= \bar{c} \left[\frac{\Theta}{2} \left\{ \left(1 + \xi \right) - \left(1 - \xi \right) \cos\theta \right\} - \lambda \right] \tag{22}$$

where

$$\bar{c} = \frac{ac}{2(R_2 - R_1)} \tag{23}$$

$$\xi = R_1 / R_2 \tag{24}$$

$$\xi_r = R_r / R_2 \tag{25}$$

$$\xi_t = R_t / R_2 \tag{26}$$

$$h_s = 2sh/(R_2 - R_1) \tag{27}$$

and

$$\lambda = U_c / \Omega R_2 \tag{28}$$

Assuming the vertical velocity of rolled-up vortices is equal to the average induced velocity plus the climb velocity, the vertical distance between successive vortices is given by

$$h = \frac{(U_c + v_0) 2\pi}{\Omega b} \tag{29}$$

Selecting finite values for m and s say M and N respectively, equation (22) yields a set of linear simultaneous algebric equations from which one can evaluate the Fourier coefficients. After this, calculation of induced velocity and thrust coefficient is a simple matter. From equations (9), (15), (16), (24) and (28) the induced velocity is given by

$$\frac{v_i}{\Omega R_2} = \Theta \left[\left(\frac{1+\xi}{2} \right) - \left(\frac{1-\xi}{2} \right) \cos\theta \right] - \lambda - \frac{2(R_2 - R_1)}{ac} \sum_{m=1}^{M} A_m \sin m\theta \tag{30}$$

and from equations (1), (15) and (5b) the blade loading distribution is

$$\frac{dL}{dr} = \rho \Omega^2 R_2 (R_2 - R_1) \left[\left(\frac{1+\xi}{2} \right) - \left(\frac{1-\xi}{2} \right) \cos\theta \right] \sum_{m=1}^{M} A_m \sin m\theta \tag{31}$$

Integrating the above equation along the blade, multiplying by the number of blades and dividing by $\rho A \Omega^2 R_2^2$ we get the thrust coefficient of the rotor

$$C_T = \frac{(1-\xi)^2 b}{4} \left[\frac{1+\xi}{2} A_1 - \frac{1-\xi}{4} A_2 \right] \tag{32}$$

On substituting λ equal to zero in the above analysis we obtain the results for the hovering case.

5. NUMERICAL EXAMPLES

An iterative process is used to calculate induced velocity and thrust. An arbitrary downwash distribution and thrust coefficient are first assumed. The wake geometry is generated using these initial values. Then we formulate a set of simultaneous algebraic equations with the Fourier coefficients as unknowns. These equations are solved by using the standard numerical algorithm based on Crout's factorisation method. From known Fourier coefficients, new values of induced velocity and thrust coefficient are calculated thus completing the first iterative cycle. The process, which is shown in Figure 10, is repeated until convergence of v_0 and C_T.

Calculations were performed to determine the induced velocity of two helicopter rotors. The aircraft is assumed to be in steady hovering flight. The important parameters for these rotors are given in Table 3.

TABLE 3
Important Parameters for the Two Rotors

Rotor	Radius (m)		Chord (mm)	Tip Speed	No. of Blades,	Blade Root	Linear Twist	Aero-Foil
	R_1	R_2	c	(r/min)	b	Pitch	Rate	Section
S·58[20]	1·37	8·50	417·0	222	4	13·9°	−8·0°	NACA 0012
Model Rotor[11]	0·088	0·58	51·0	1400	3	15·0°	−8·0°	NACA 0012

The weight of the model aircraft was about 6·8 kg. The weight of the S·58 aircraft varied between 5085 and 5360 kg. In the numerical calculations M and N were set to 20 and 12 respectively.[11] In both cases, lift slope is taken to be 5.73. From published experimental results[9,10] C_T was initially assumed to be 0·005. An initial value of v_0 was calculated using the momentum theory equation[2]:

$$v_0 \quad \tfrac{1}{2}\left[-U_c^2 + (U_c^2 + 2W_e/\rho\pi R_2^2)^{\frac{1}{2}}\right] \tag{33}$$

With the above input data, the iterative process is commenced. Calculated values of v_0 are plotted as a function of iteration number in Figure 11. As we can see from this figure, the solution converges very rapidly.

6. COMPARISON WITH FLIGHT DATA AND WITH OTHER THEORIES

The results shown in Figure 12 indicate that the incorporation of wake contraction significantly alters the radial distribution of induced velocity. This is particularly true in the blade tip region where the rolled-up vortex passes close to the blade. Comparison of calculated values with the experimental data is limited by the amount of data available. In fact there are no experimental data on induced velocity in the rotor plane at the present time. Hence computed blade loading is compared with measured blade loading[20] in Figure 13. Here once again we see the effect of wake contraction on the results. One should be cautious in comparing the present mathematical model with other theories, as all theories necessitate many simplifying assumptions. Therefore any comparison would rest upon the significance of the simplifying assumptions and how they affect the calculated values. Figure 15 shows a comparison with Jenney, Olson and Landgrebe's sophisticated mathematical model. The results compare well over the greater part of the blade span except near 80% of the blade radius. This could possibly be due to the simplification of the wake representation by planar rather than curved surfaces.

Results presented in Figures 12–14 also compare the present theory with Willmer's theory and flight data. Included in these figures are the calculation both with and without wake contraction. It can be seen from Figure 13 that the present method more closely predicts the blade loading in the tip region where the loading is very high. This is mainly due to the incorporation of wake contraction.

7. CONCLUDING REMARKS

The method described provides a rapid, computer-oriented, numerical technique for evaluation of rotor downwash. Results presented for two different rotors indicate that the variation of induced velocity along the radius of the rotor is highly non-linear. Correlation of the computed and measured results is quite good, considering the simple wake geometry used.

REFERENCES

1. Landgrebe, A. J. and Cheney, Jr. M. C. — Rotor wakes–Key to Performance Prediction. AGARD conference on Aerodynamics of Rotary wings. Marseilles, France, Sept. 1972.
2. Gessow, A. and Myers, Jr. G. C. — Aerodynamics of the Helicopter. The Macmillan Company, New York, 1952.
3. Crimi, P. — Theoretical Prediction of the Flow in the Wake of a Helicopter Rotor. CAL Report No. BB-1994-s-1, Sept. 1965.
4. Landgrebe, A. J. — An Analytical Method for Predicting Rotor Wake Geometry. JAHS, vol. 14, No. 4, Oct. 1969.
5. Clark, D. R. and Leiper, A. J. — The Free Wake Analysis: A Method for the Prediction of Helicopter Rotor Hovering Performance. JAHS, Vol. 15, No. 1, Jan. 1970.
6. Miller, R. H. — Rotor Blade Harmonic Air Loading. AIAA Journal, Vol. 2, No. 7, July 1964.
7. Piziali, R. A. — A Method for the Solution of the Aeroelastic Response Problems for Rotating Wings. J. Sound and Vibration, Vol. 4, No. 3, 1966.
8. Gray, R. B. — On the Motion of the Helical vortex Shed From a Single-Bladed Hovering Model Helicopter Rotor and its Application to the Calculation of the Spanwise Aerodynamic Loading. Princeton Uni. Aero Eng. Dept. Report No. 313, Sept. 1955.
9. Landgrebe, A. J. — The Wake Geometry of a Hovering Helicopter Rotor and its Influence on Rotor Performance. JAHS, vol. 17, No. 2, Oct. 1972.
10. Kocurek, J. D. and Tangler, J. L. — A Prescribed Wake Lifting Surface Hover Performance Analysis. AHS 32 V STOL Forum, May 1976.
11. Jenney, D. S., Olson, J. R. and Landgrebe, A. J. — A Reassessment of Rotor Hovering Performance Prediction Methods. AHS 23rd Annual National Forum, May 1967.
12. Young, C. — The Prediction of Helicopter Rotor Hover Performance using a Prescribed Wake Analysis, RAE, TR-74078, August 1974.
13. Cook, C. V. — Rotor Performance Prediction in Hover. Westland Helicopters Limited, Research Paper 357, Nov. 1968.
14. Ormiston, R. A. — An Actuator Disc Theory for Rotor Wake Induced Velocities. AGARD Conference on Aerodynamics of Rotary Wings, Marseilles, France, Sept. 1972.
15. Willmer, M. P. — The Loading of Helicopter Rotor Blades in Forward Flight. British ARC R and M No. 3318, 1963.
16. Bramwell, A. R. S. — Helicopter Dynamics. Edward Arnold, London, 1976.
17. Milne-Thomson, L. M. — Theoretical Aerodynamics. Macmillan and Company Limited, London, 1948, Sec. 4.71, 11.201.
18. Loewy, R. G. — A Two-Dimensional Approximation to the Unsteady Aerodynamics of Rotary Wings. J. Aero. Sci., Vol. 24, No. 2, Feb. 1957.

19. Glauert, H. The Elements of Aerofoil and Airscrew Theory. First Edition, University Press, Cambridge, 1937, Sec. 10.32, 12.4, 13.14.

20. Scheiman, J. A Tabulation of Helicopter Rotor-Blade Differential Pressures, Stresses, and Motions as Measured in Flight. NASA TM X-952, March 1964.

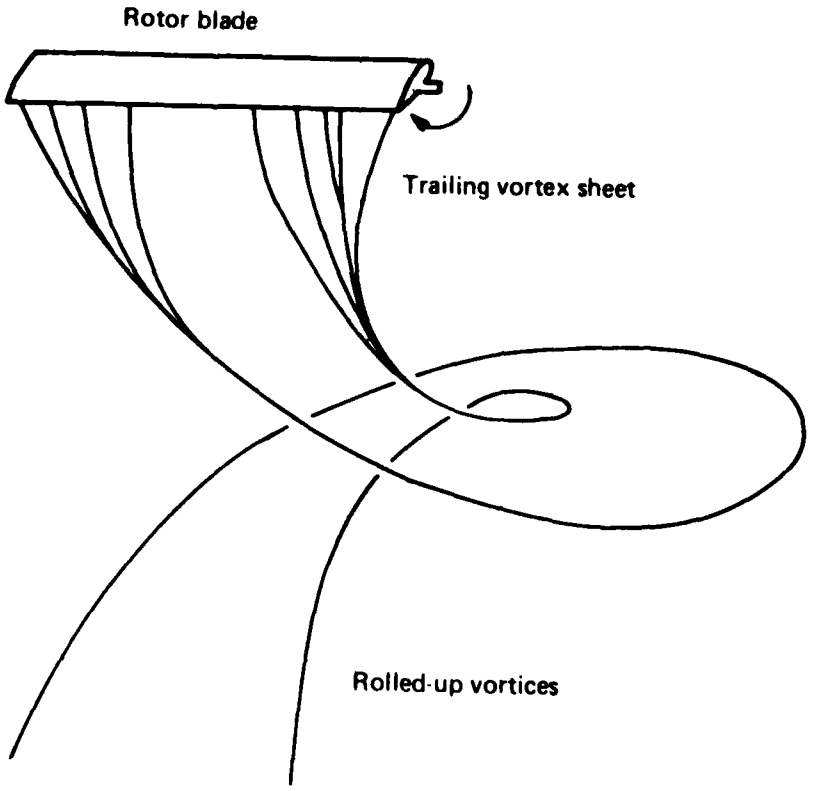

FIG. 1. ROTARY WING WAKE GEOMETRY

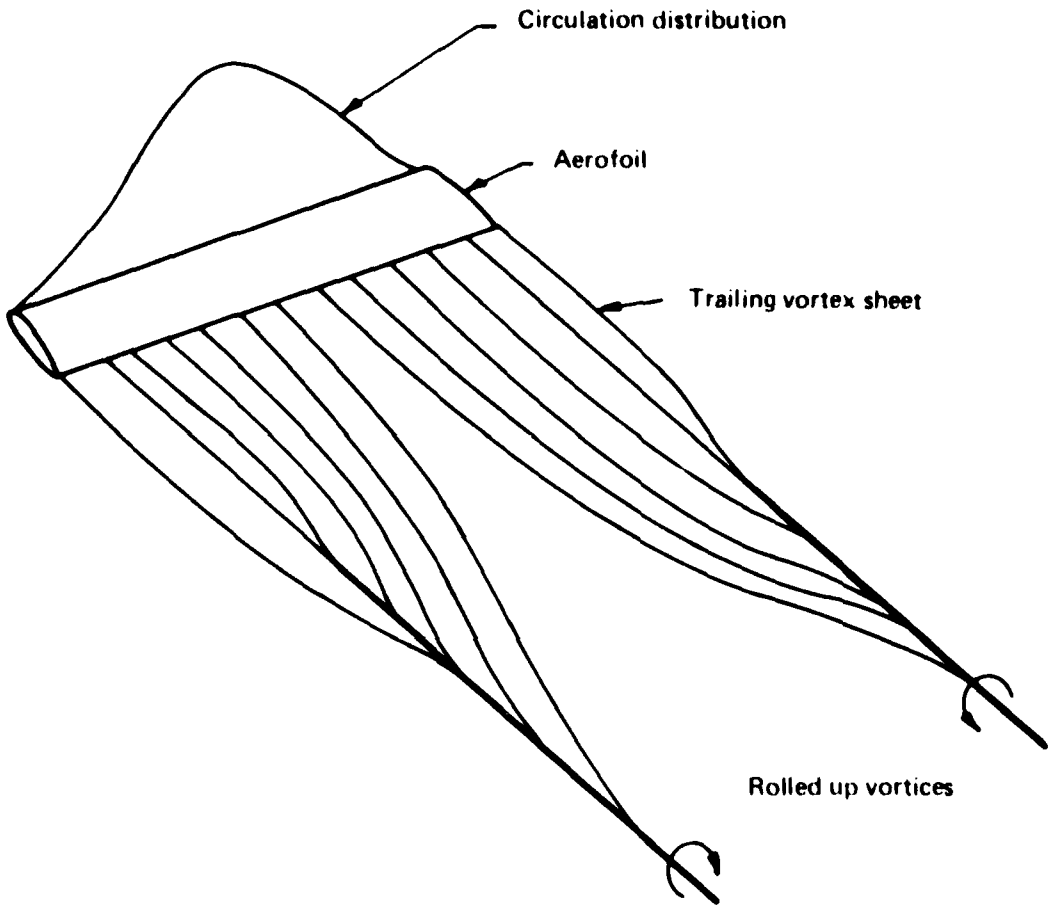

FIG. 2. FIXED WING WAKE GEOMETRY

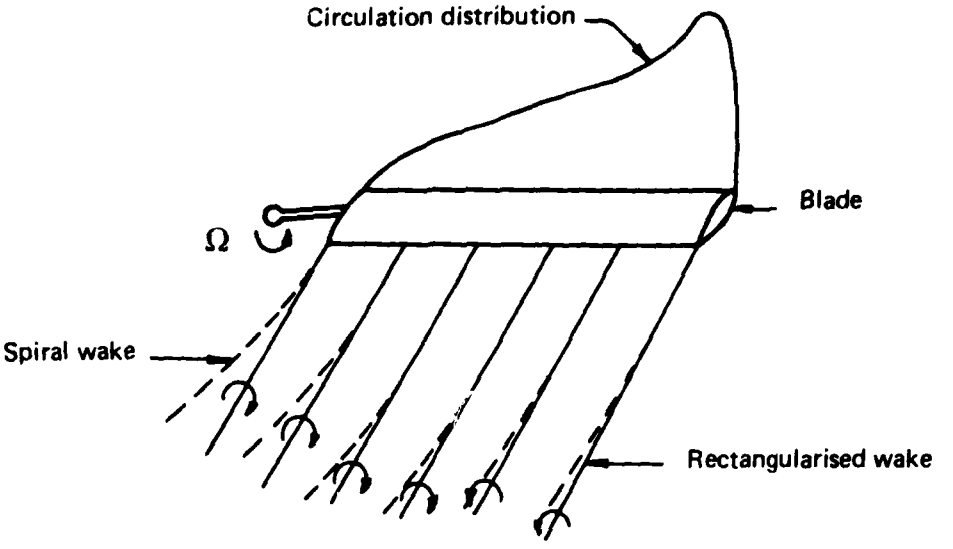

FIG. 3. RECTANGULARIZATION OF ROTARY WING WAKE

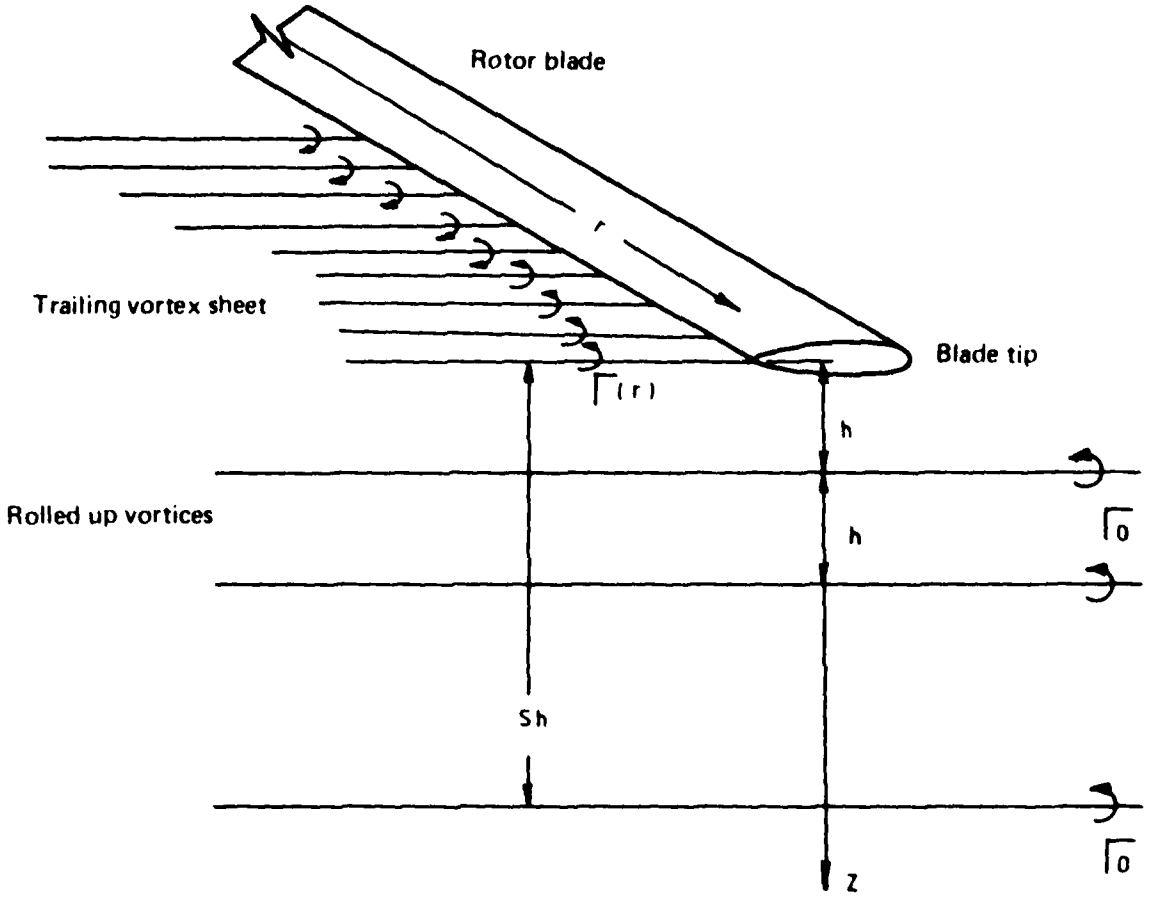

FIG. 4. TRAILING VORTEX SHEET AND ROLLED-UP VORTICES NEAR BLADE TIP

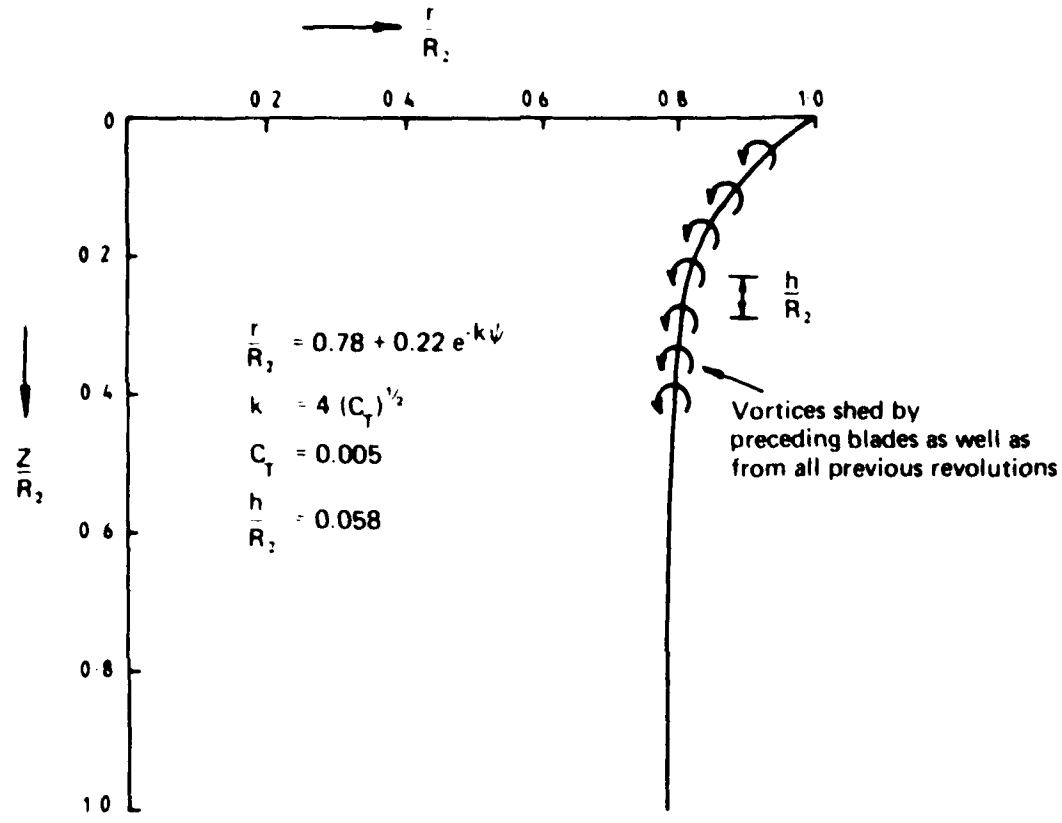

FIG. 5. CONTRACTION OF ROTOR WAKE

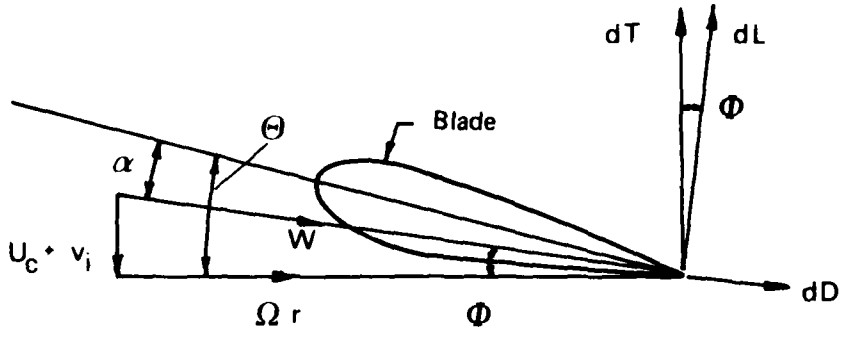

FIG. 6. FORCE AND VELOCITY COMPONENTS ON BLADE ELEMENT

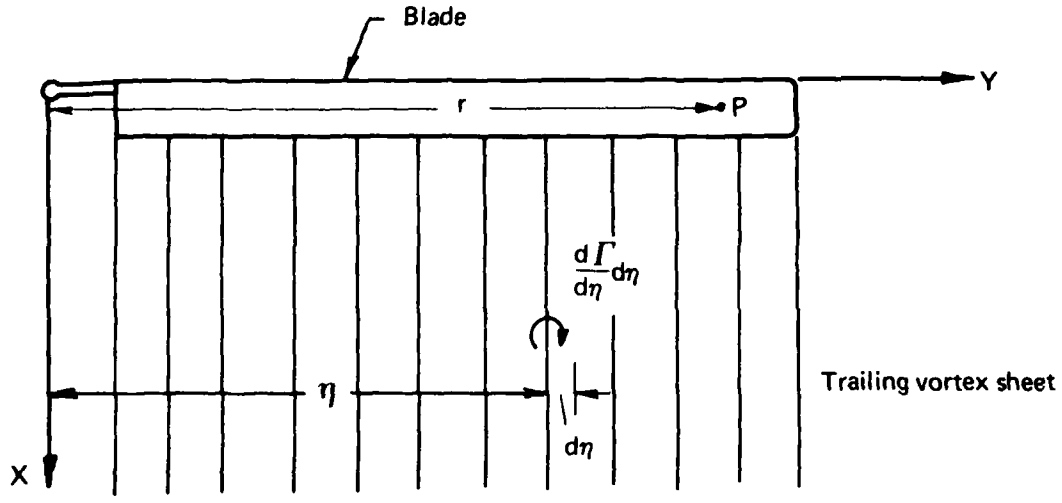

FIG. 7. VORTEX SHEET BEHIND THE ROTOR BLADE

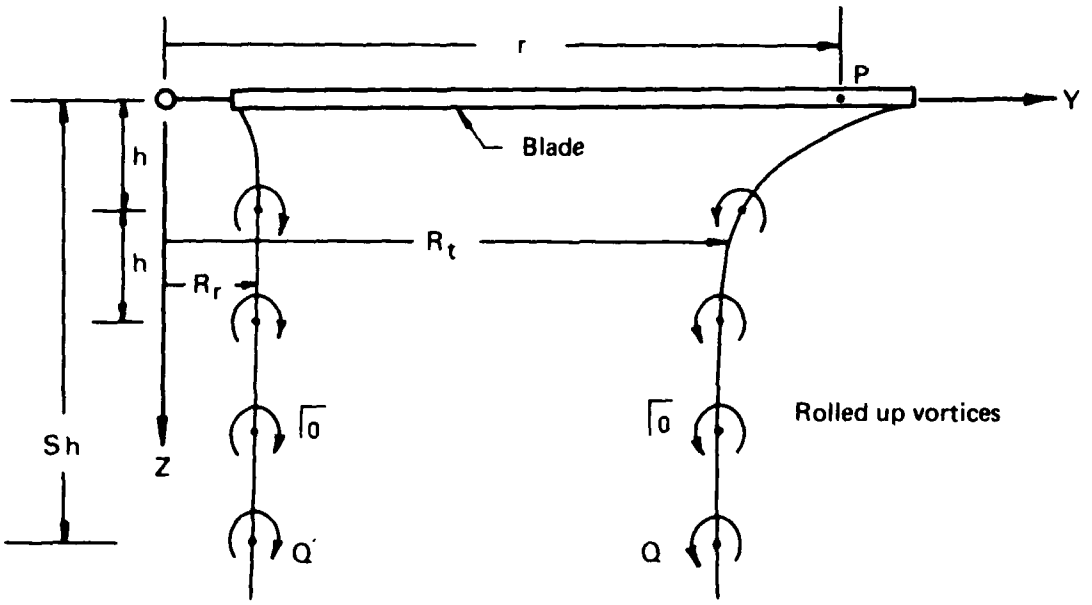

FIG. 8. ROLLED UP VORTICES BELOW THE ROTOR BLADE

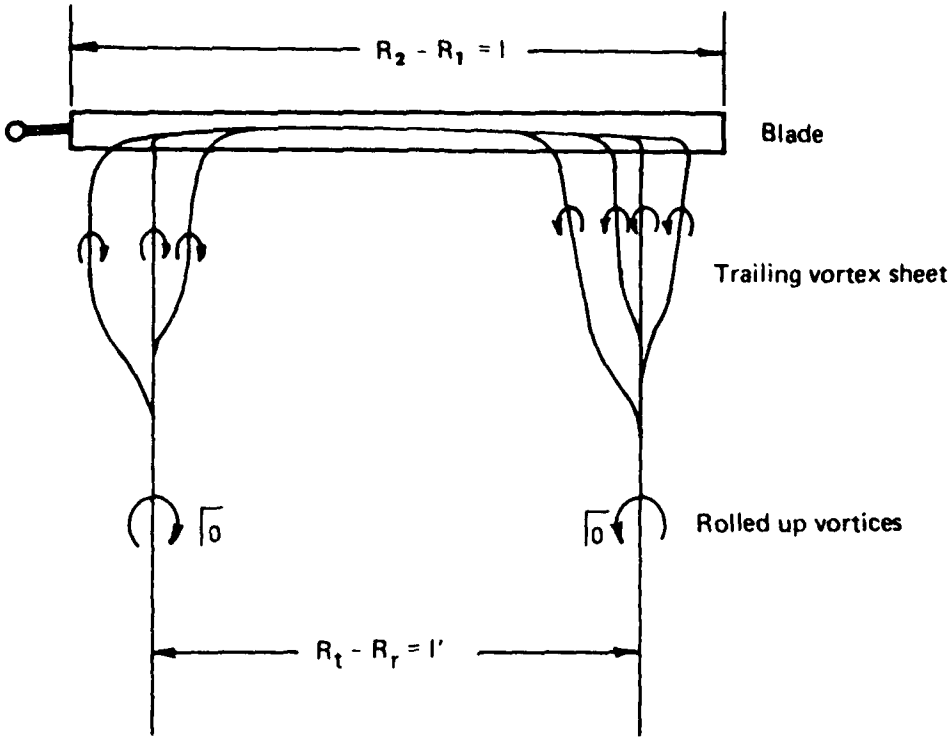

FIG. 9. REPRESENTATION OF TRAILING VORTICES

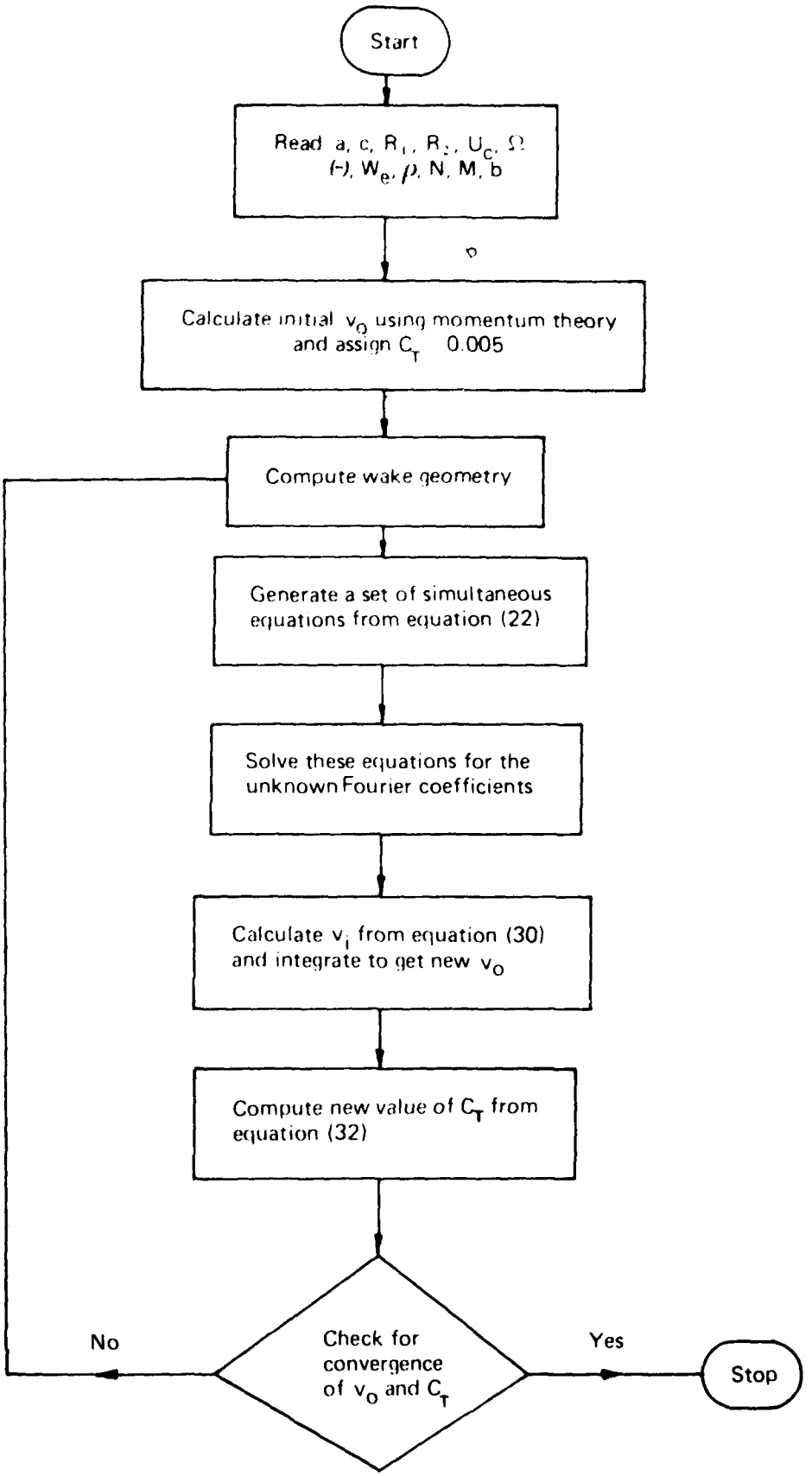

FIG. 10. COMPUTATIONAL FLOW CHART

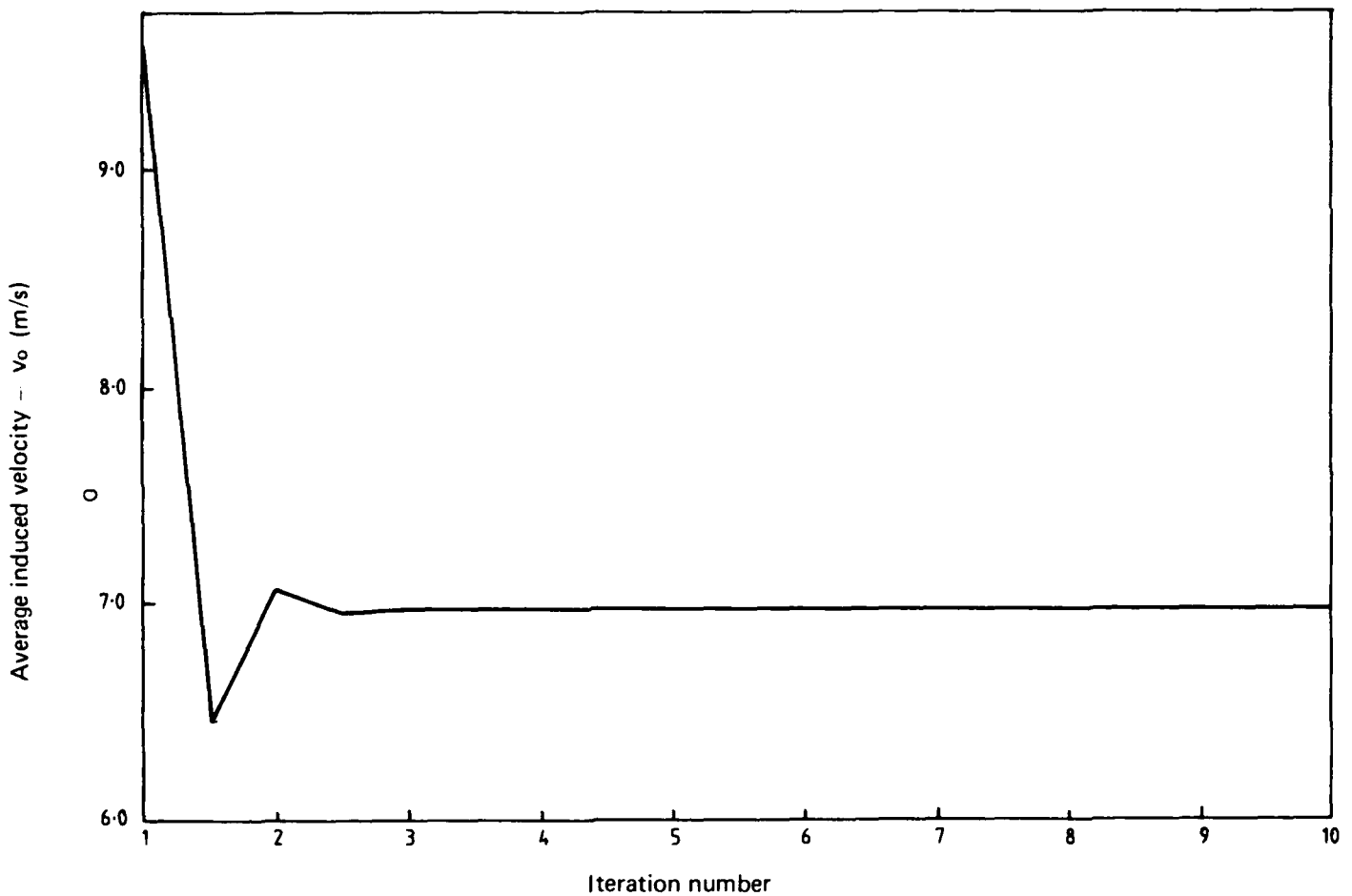

FIG. 11. AVERAGE INDUCED VELOCITY vs. INTERATION NUMBER – S.58 ROTOR

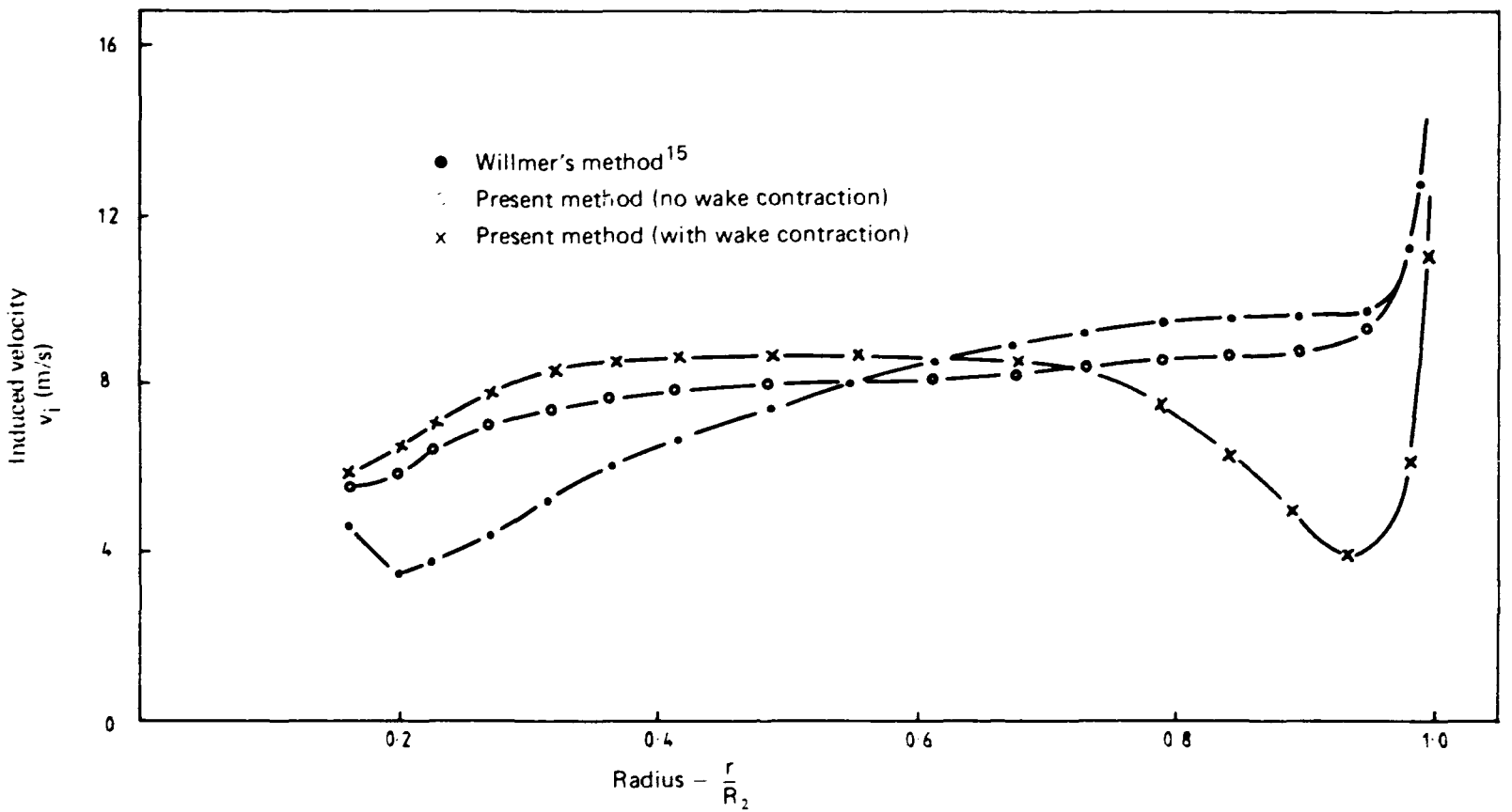

FIG. 12 VARIATION OF INDUCED VELOCITY WITH RADIUS – S.58 HELICOPTER

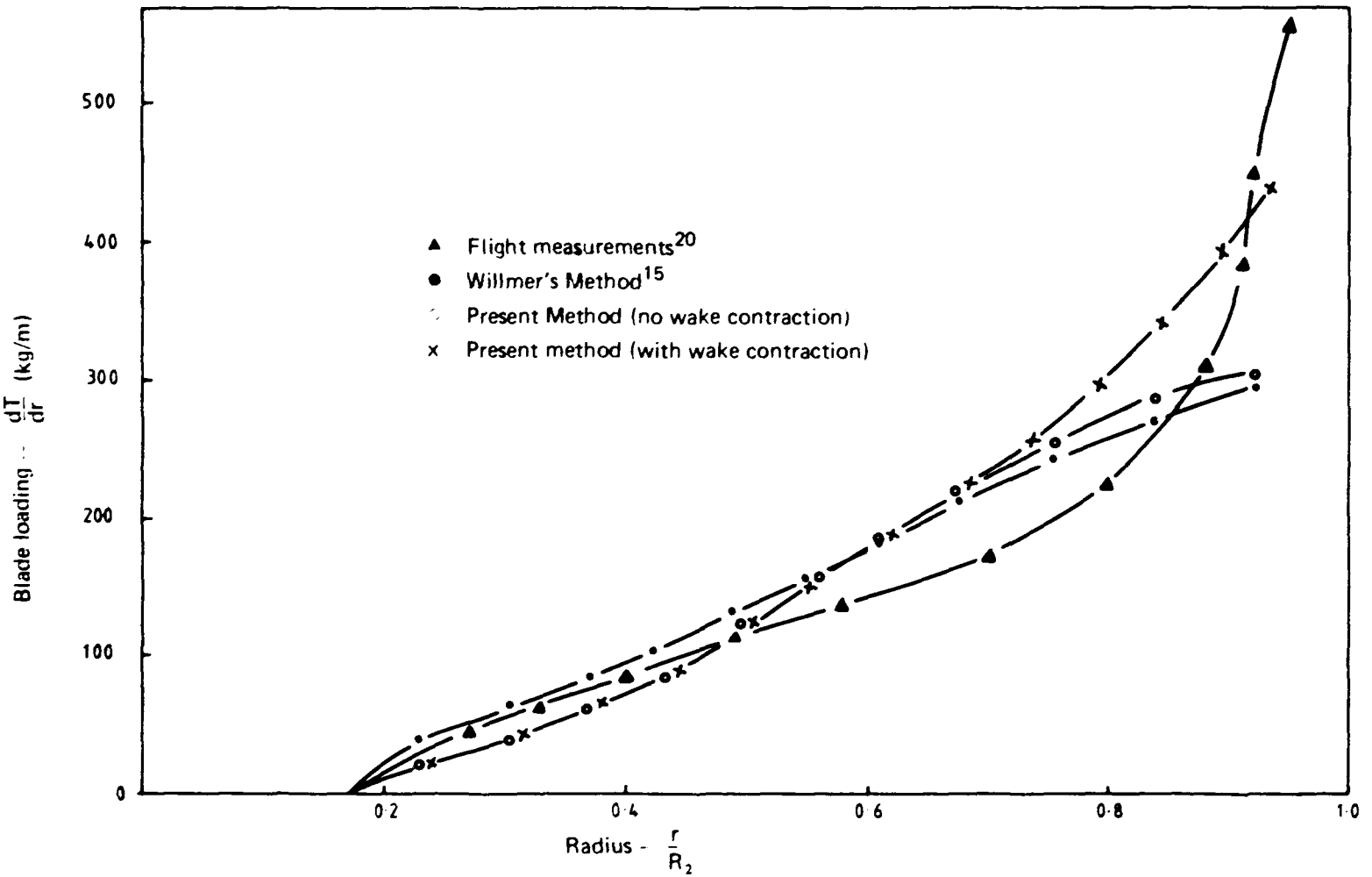

FIG. 13. VARIATION OF BLADE LOADING WITH SPAN – S.58 HELICOPTER

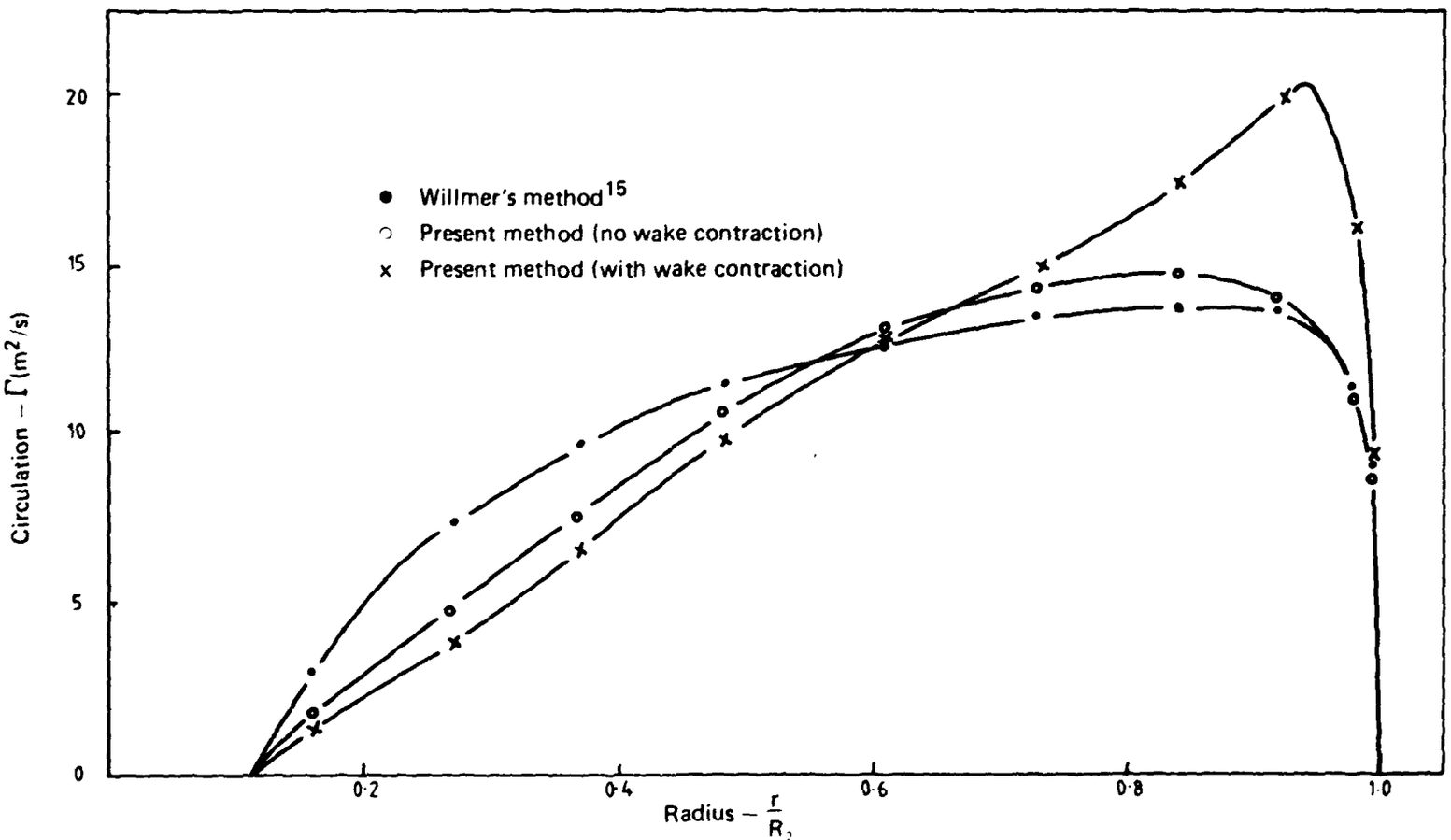

FIG. 14. VARIATION OF BLADE CIRCULATION WITH SPAN – S.58 HELICOPTER

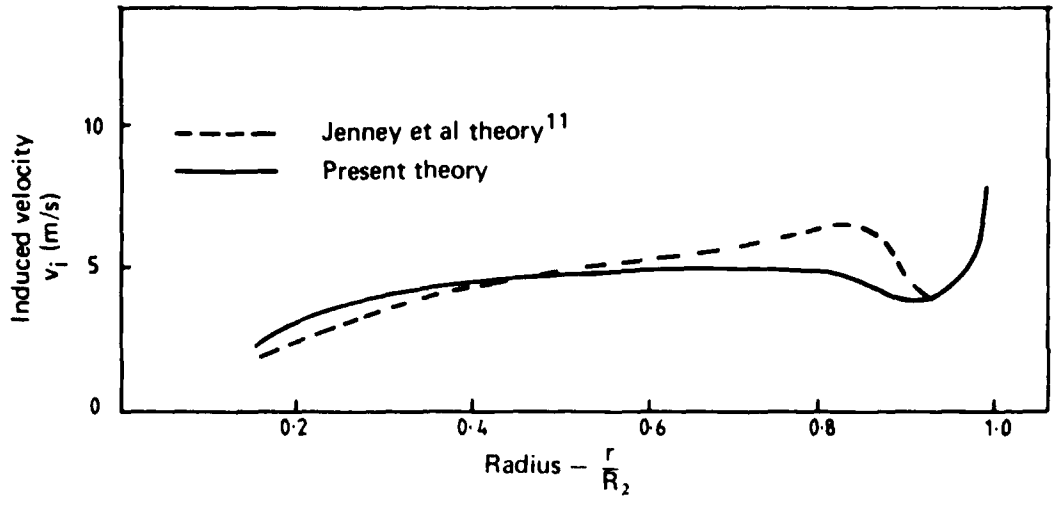

(a) Induced velocity

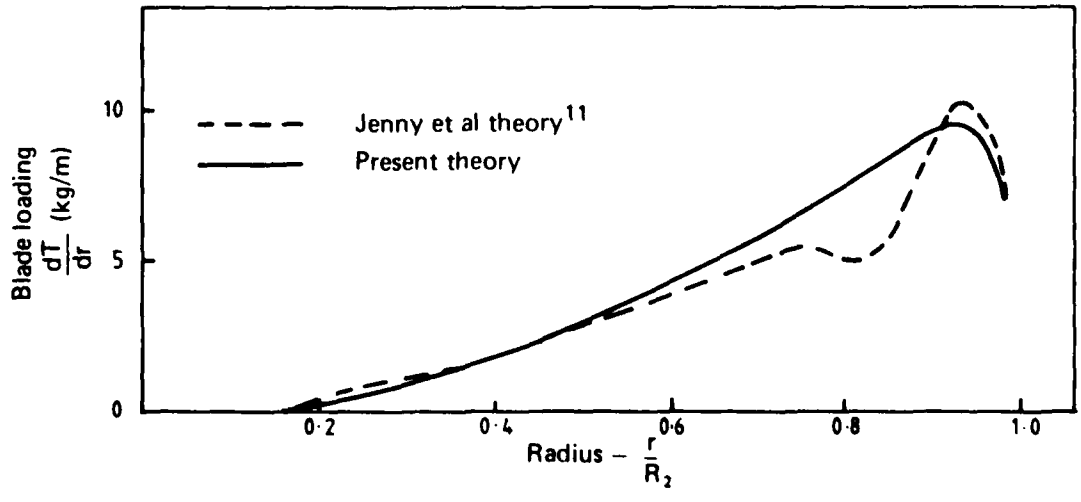

(b) Blade loading

FIG. 15. COMPARISON OF CALCULATED VALUES WITH JENNEY, OLSON AND LANDGREBE'S RESULTS FOR MODEL ROTOR

DOCUMENT CONTROL DATA SHEET

Security classification of this page: Unclassified

1. Document Numbers
   (a) AR Number:
   AR-001 335
   (b) Document Series and Number:
   Aerodynamics Report 150
   (c) Report Number:
   ARL Aero Report 150

2. Security Classification
   (a) Complete Document:
   Unclassified
   (b) Title in isolation:
   Unclassified
   (c) Summary in isolation:
   Unclassified

3. Title: PREDICTION OF HELICOPTER ROTOR DOWNWASH IN HOVER AND VERTICAL FLIGHT

4. Personal Author(s):
   K. R. Reddy

5. Document Date:
   January, 1979

6. Type of Report and Period Covered:

7. Corporate Author(s):
   Aeronautical Research Laboratories

8. Reference Numbers
   (a) Task:

   (b) Sponsoring Agency:

9. Cost Code:
   51 7740

10. Imprint:
    Aeronautical Research Laboratories,
    Melbourne

11. Computer Program(s)
    (Title(s) and language(s)):

12. Release Limitations (of the document)
    Approved for public release

12-0. Overseas:	N.O.		P.R.	1	A		B		C		D		E	

13. Announcement Limitations (of the information on this page):
    No limitation

14. Descriptors:

		15. Cosati Codes:
Helicopters	Computation	0103
Rotary wings	Wakes	1201
Downwash	Vortices	2004
Hovering	Vertical flight	

16.

ABSTRACT

A method is presented for the calculation of rotor downwash in hovering and vertical flight. The blade is represented by a lifting line. The rotor wake is simulated by a vortex sheet and a series of rolled-up root and tip vortices, similar in form to that of a classical fixed-wing. The concept of rectangularization of the rotor wake is used in obtaining a formula for the normal component of induced velocity. Wake contraction based on experimental data is introduced into the calculations. Numerical calculations have been performed for two rotor configurations viz. S-58 and a model rotor. Computed induced velocities and blade loadings are compared with the available flight data. The comparison shows the present simple method yields satisfactory results.

DISTRIBUTION

	Copy No.
AUSTRALIA	
Department of Defeuce	
Central Office	
Chief Defence Scientist	1
Deputy Chief Defence Scientist	2
Superintendent, Science and Technology Programs	3
Defence Library	4
Joint Intelligence Organisation	5
Assistant Secretary, DISB	6–21
Australian Defence Scientific & Technical Representative (UK)	22
Counsellor, Defence Science (USA)	23
Aeronautical Research Laboratories	
Chief Superintendent	24
Superintendent, Aerodynamics Division	25
Divisional File, Aerodynamics Division	26
Author: K. R. Reddy	27
Library	28
Aerophysics Group (D. C. Collis)	29–33
N. Matheson	34
D. A. Lemaire	35
P. A. Farrell	36
Materials Research Laboratories	
Library	37
Defence Research Centre, Salisbury	
Library	38
RAN Research Laboratory	
Library	39
Navy Office	
Naval Scientific Adviser	40
DNAE (Mr A. C. Marshall)	41
Army Office	
Army Scientific Adviser	42
Royal Military College	43
Air Force Office	
Air Force Scientific Adviser	44
Aircraft Research and Development Unit	45
Engineering (CAFTS) Library	46
D. Air Eng.	47
Department of Productivity	
Government Aircraft Factories, Library	48
Department of Transport	
Secretary/Library	49
Airworthiness Group (Mr K. O'Brien)	50

Statutory, State Authorities and Industry

CSIRO Mechanical Engineering Division (Chief)		51
Qantas, Library		52
Trans Australia Airlines, Library		53
SEC Herman Research Laboratory, Librarian, Vic.		54
Ansett Airlines of Australia, Library		55
Commonwealth Aircraft Corporation (Manager of Engineering)		56
Hawker de Havilland Pty Ltd, Librarian, Bankstown		57
Rolls Royce of Australia Pty Ltd (Mr Mosley)		58

Universities and Colleges

Adelaide	Barr Smith Library	59
	Professor of Mechanical Engineering	60
Australian National	Library	61
Flinders	Library	62
James Cook	Library	63
La Trobe	Library	64
Melbourne	Engineering Library	65
	Professor Whitton, Mechanical Engineering	66
Monash	Library	67
Newcastle	Library	68
New England	Library	69
New South Wales	Physical Sciences Library	70
	Professor R. A. A. Bryant	71
Queensland	Library	72
Sydney	Mr E. D. Poppleton, Aeronautical Engineering	73
	Professor R. I. Tanner, Mechanical Engineering	74
	Professor B. W. Roberts, Mechanical Engineering	75
Tasmania	Engineering Library	76
Western Australia	Library	77
	Professor Allen-Williams, Mechanical Engineering	78
RMIT	Library	79
	Mr H. Millicer, Aeronautical Engineering	80
	Mr Pugh, Mechanical Engineering	81

CANADA

NRC, National Aeronautical Establishment, Library		82

Universities

McGill	Library	83
Toronto	Institute for Aerospace Studies	84
Memorial University of Newfoundland, Professor D. V. Reddy		85

FRANCE

AGARD, Library	86
Gaz de France, Library	87

GERMANY

ZLDI	88

INDIA

Civil Aviation Department (Director)	89
Defence Ministry, Aero Development Establishment, Library	90
Hindustani Aeronautics Ltd, Library	91
Indian Institute of Science, Library	92
Indian Institute of Technology, Library	93
National Aeronautical Laboratory (Director)	94

UNITED STATES OF AMERICA

NASA Scientific and Technical Information Facility		132
American Institute of Aeronautics and Astronautics		133
Applied Mechanics Reviews		134
Boeing Co. Head Office		135
Lockheed Aircraft Co. (Director)		136
McDonnell Douglas Corporation (Director)		137
United Technologies Corporation, Fluid Dynamics Laboratories		138
Universities and Colleges		
Florida	Aero. Engineering Department	139
Harvard	Professor A. F. Carrier, Applied Mathematics	140
	Dr S. Goldstein, Applied Physics	141
Johns Hopkins	Professor S. Corrsin, Mechanical Engineering	142
Stanford	Department of Aeronautics Library	143
Brooklyn Institute of Polytechnology	Polytech Aeronautical Labs Library	144
California Institute of Technology	Guggenheim Aeronautical Labs Library	145
Massachusetts Inst. of Technology	Library	146
Georgia Institute of Technology	Professor R. B. Gray, Aerospace Engineering	147
Spares		148–157